CONF-8809288 1

INTERACTION OF MULTIPLY CHARGED IONS WITH SOLID SURFACES

CONF-8809288--1

DE89 005112

C. C. Havener, K. J. Reed [▽], K. J. Snowdon[♠], D. M. Zehner, and F. W. Meyer
Oak Ridge National Laboratory, Oak Ridge, Tennessee 37831-6372, USA

ABSTRACT

The observation of the decay of inner-shell vacancies can serve as an excellent probe of the neutralization of multicharged ions during their approach to a metal surface. Several recent experiments that have measured electrons emitted during this neutralization are discussed. Measurements of the total electron yield for incident ions with inner-shell vacancies first showed marked differences from the yield observed for lower charge states and indicated the need for further investigations. Measurements of the emitted electron energy distributions have led to a qualitative understanding of the timescales of the neutralization process. For incident ions with high enough energies, projectile inner-shell vacancies have been observed to survive the neutralization process above the surface and then to be transferred to target atoms in close collisions. The inner-shell reactions occuring in such close collisions are analogous to those that have been observed in ion-atom and ion-foil collisions. Recent measurements of angular distributions of the electrons emitted due to the decay of target vacancies created during the interaction show evidence of the projectile penetrating several layers below the surface.

DISCLAIMER

INTRODUCTION

With the availability of advanced ion sources such as the Electron Cyclotron Resonance (ECR) type sources,[1] there have been recent experimental investigations to test the semiempirical models that were previously established for lower charge state ions interacting with surfaces and extended to include highly charged ions containing inner-shell vacancies. The electrons emitted due to the significant potential energy contained in these ions are excellent probes of the neutralization process.

In general, electron emission during ion-surface interactions includes contributions directly due to the dissipation of the potential energy of the incident ion ("potential" emission), as well as those due to transfer of kinetic energy of the projectile to metal electrons ("kinetic" emission[2,3]) . In the past, potential emission has been studied by performing measurements with incident ion velocities below the threshold for kinetic emission ($\approx 1 \times 10^5 m/s$), by estimating and then subtracting out the kinetic emission from the total electron yield, or by selectively observing only high energy electrons (the energy of electrons ejected by kinetic emission is typically $\leq 50eV$). Alternatively, if the incident ion approaches the surface at low enough grazing angles for planar channeling (specular reflection) to occur,[4] then the ion will stay above the surface, thereby minimizing energy exchange with the metal electrons, and consequently also kinetic emission. Electrons emitted in this regime should thus be mainly due to potential emission. Recently,[5] for lower charge states, the difference in statistics of the two emission processes has been used to distinguish the two contributions.

In order for the neutralization of the ion to be complete, the ion must spend sufficient time above the surface. Experimentally, the time above the surface is maximized by either approaching the surface at low energies or at grazing angles of incidence. If inner-shell vacancies survive the neutralization process, then they may be transferred to surface or subsurface atoms in close collisions. Such inner shell processes are analogous to the ones proviously observed in ion-atom[6] and ion-foil[7] measurements.

The following discussion will focus on a few of the more recent experiments which

have observed the electrons emitted as multicharged ions interact with metal surfaces and show how these measurements have led to a better understanding of the neutralization process. For a more comprehensive discussion the reader is directed toward several recent reviews.[8,3,9,10]

MEASUREMENTS OF TOTAL YIELD

Most of the experiments performed so far have measured the total electron yield, γ, for a wide variety of projectiles incident on metal surfaces. Several early observations of electron yield as a function of projectile charge state established a linear relationship, $\gamma = kW_q$, between the electron yield and the total neutralization energy W_q, defined as $W_q = \sum_{i=1}^{q} I_{i-1,i}$, where $I_{i-1,i}$ is the ionization potential of the ion with charge (i-1)+.

These observations are consistent with the theoretical model proposed by Arifov et al.,[11] in which the primary mechanism of neutralization is multiple transfer of target valence electrons to high lying projectile excited states, which subsequently relax via several one-center Auger decays, emitting electrons with an energy of 15-30 eV. More recent work[12,13] measured the energy dependence of these proportionality constants, k. Quite remarkably, they found that for incident ion velocities $v \leq 4.0 \times 10^4 m/sec$, and ions ranging with charge up to N^{6+}, Ne^{7+}, Ar^{12+}, and Kr^{11+}, γ was observed to have a linear dependence with W_q. However, when the velocity of the incident ion was increased, all observed k gradually decreased. For those ions which contained a L-shell vacancy (e.g., Ar^{q+}, $q \geq 9$) or a K-shell vacancy (e.g., N^{6+}), k was found to be significantly reduced at the higher energies. A qualitative understanding of these results was obtained by considering the timescales of the multiple-step ion-neutralization model. It was speculated[12,13] that at the higher energies the inner-shell vacancies survived until close collisions with the surface atoms where electron emission is somehow less efficient. However, these total γ measuremets do not contain direct evidence of the fate of these inner-shell vacancies. To gain more information

we turn to measurements of the electron energy distributions of the electrons emitted during the interaction with the surface.

MEASUREMENTS OF ELECTRON ENERGY DISTRIBUTIONS

The electron energy distributions measured by various groups[14-16] for multicharged ions as they approach metal surfaces have led to an increased understanding of the neutralization process. For incident projectiles containing K and L vacancies, characteristic KLL and LMM Auger electrons have been identified in the measured electron energy distributions. As an example, Fig. 1 shows the electron energy distribution for 60 keV $N^{4,5,6+}$ ions incident on Au at 5° grazing incidence (see inset). Most of the electrons are emitted at energies below 50 eV due to an unknown mixture of kinetic and potential emission. The spectra for the H- and He- like ions, N^{6+} and N^{5+}, respectively, show a broad feature around 350 eV which has been identified[17] as being due to the filling of the initial K-shell vacancy via KLL Auger emission. The K vacancy for the He-like ions comes from the metastable $(1s2s)^3S$ fraction of the beam. For the Li-like projectiles which have no metastable states, in general,[18] and which do not contain any K-vacancies in particular, the peak is no longer present. By a comparative analysis of these spectra, the metastable fraction of the N^{5+} beam has been determined.[19] Metastable fractions have also been determined[19,16] for various other ion beams containing K- and L-shell vacancies. However, the possibility of projectile inner-shell excitation mechanisms[20,10] needs to be considered before metastable fractions are inferred from such measurements.

For the electron energy distributions obtained with analysers characterized by large angular acceptance[14,16,17,20,19] (e.g., as in Fig. 1), the possibility of large Doppler broadening precludes extersive analysis of the observed peaks. Electron energy distributions which have been measured using analysers with a small angular acceptance show well defined Doppler shifts of the LMM and KLL peaks for Ar^{9+} + W [15] and for O^{7+} + Au,[10] respectively. These shifts confirmed that the electrons observed were

due to the decay of the inner-shell vacancies on the ion's approach to the surface.

TIMESCALES OF THE NEUTRALIZATION PROCESS

The various timescales[21,22] of the neutralization process have been explored experimentally by varying the velocity of the incident beam[15] or the angle of incidence[10] to the surface, both methods essentially changing the time interval the ions spend above the surface. Fig. 2 shows the velocity dependence of the LMM peak observed[15] for Ar^{9+} on W due to the decay of the L vacancy on the incident ion. This peak is observed to be shifted $\approx$ 7 eV to higher energies compared to that observed in gas phase collisions. The observed shift has been explained[23] as resulting from the decay occuring in a completely neutralized projectile in the presence of an induced surface image charge. The decrease of the peak intensities with increasing collision energy is understood in terms of the timescales of the neutralization process. At a critical distance above the surface (estimated in Ref.21) to be 2q + 7 a.u., where q is the charge of the incident ion), multiple resonant neutralization from the valence band of the metal occurs (on a timescale on the order of 5 x 10^{-16} s),[22] which populates highly excited Rydberg levels of the incident ion. Concurrent with the continual filling of the higher levels, electrons cascade down to (in this case) the M shell. As soon as at least two electrons have arrived there, LMM transitions can occur. Model calculations[23] using estimated rates for filling the M shell as a function of the distance above the surface and a constant rate of the subsequent LMM Auger decay of the L vacancy successfully reproduced the observed trend of the spectra with incident ion energy.

Fig. 3 shows the electron spectra measured[10] for 70 keV O^{7+} + Au with incident angles between 10 and 80°. Assuming that neutralization of the multicharged ion begins at a distance of $\approx$2q+7 a.u., the resultant above-surface neutralization times cover the range of 1-7 x 10^{-15} sec, the shortest time corresponding to the largest angle of incidence (80°). As can be seen in the figure, the position of the KLL peak does not change with interaction time, while the height of the peak decreases monotonically

with decreasing interaction time. Using the codes of Cowan,[24] configuration-averaged KLL transition energies and KLL Auger rates were calculated[10] for different charge states of oxygen. The fastest decay rate ($\geq 2 \times 10^{14}$ s^{-1}) was found for neutral O (with a "superfilled" L shell). Since the KLL Auger peak is centered around the energy corresponding to the decay of neutral oxygen, it was argued that the filling rates of the L shell must therefore be faster than the KLL decay time. At 10° angle of incidence, the interaction corresponds to about 1.2 KLL decay lifetimes, while at 80°, the available time corresponds to only about 0.2 KLL decay lifetimes. This explains the gradual disappearance of the observed KLL peaks with increasing angle of incidence. The larger width of the KLL decay relative to what was observed for the LMM decay may indicate relatively slower filling of the L shell, allowing more KLL Auger contributions from higher charge states.

EVIDENCE OF CLOSE COLLISIONS

In addition to Auger electrons originating from the projectiles, characteristic electrons from the target have been observed.[15,14] These electrons result from Auger decay of target vacancies created during the interaction. Examples of such Auger transitions are the peaks at 70 and 220 eV in Fig. 1, corresponding to $N_{4,5}N_{6,7}V$ and $N_{6,7}VV$ transitions filling vacancies in the $N_{4,5}$ inner shells of the Au target. As is shown in the correlation diagram (see Fig. 4) constructed with the rules in Ref.,[25] a likely mechanism for the creation of these target inner shell vacancies is vacancy transfer from the projectile K-shell via a pseudocrossing of the strongly promoted molecular orbital correlating to the projectile 1s level, and the weakly demoted molecular orbital correlating to the $N_{4,5}$ levels in Au. Vacancies have also been observed,[14] for example, to be created on C which may be present as a contaminant on the surface. The vacancy production mechanism in this case is $2p\pi$ - $2p\sigma$ rotational coupling, well known and studied in ion-atom collisions,[6] which transfers an initial 2p vacancy in N to the 1s shell of C. Auger electron emission resulting from the filling of such target

vacancies is evidence for close collisions between the projectile and target atoms.

A quantitative measure of the distance of closest approach can be found in the electron energy distributions measured for F^{q+} ions ($\approx$ q $x10keV, q = 2-8$) interacting with a Cu surface at 5° grazing incidence.[20] The spectra for all charge states for incident energies $\geq$ 33 keV show a high energy feature around 625 eV which is associated with KLL Auger decay in the F projectiles. Fig. 5 shows this 625 eV peak for several incident flourine ion charge states. For H-like F^{8+} and metastable He-like F^{7+} ions, the 625 eV peak is attributed to the filling of K-shell vacancies present in the incident beam. Since Li-like ions are known not to contain K-vacancies, the observation of the peak in the spectra for F^{6+} is evidence for inner-shell vacancy production during close collisions with Cu target atoms. The mechanisms responsible for the vacancy production are understood in terms of molecular orbital diagrams calculated using the variable screening model of Eichler and Wille.[26] Fig. 6 shows the diagram for the F^{2+} - Cu system. The diagram represents the purely electronic binding energy of molecular orbitals as a function of internuclear separation. From this diagram, it can be seen that the several crossings necessary for the transfer of an initial F(2p) vacancy to F(1s) are located in the range of internuclear separations from 0.15 to 0.5 a.u., and that consequently a distance of closest approach of $\leq$ 0.15 a.u. is required in order that the vacancy transfer occur. Using the Moliere interatomic potential[4] it was shown that for energies $\leq$ 33 keV this distance of closest approach could not be reached. It was speculated[20] that the inability to access the innermost crossing might explain the disappearance of the 625 eV peak in the F^{2+} spectrum as seen in Fig. 5.

Fig. 5 also shows a more detailed view of the F KLL Auger feature at around 625 eV, together with calculated configuration-averaged KLL Auger electron transition energies for the three highest flourine charge states investigated. Comparison of these calculations with the measured KLL features gives information about the charge state of the F projectile at the time of the KLL Auger decay. As can be seen from the figure, for all three initial projectile charge states, the largest contribution to the KLL peak

comes from F ions which have been almost completely neutralized, i.e. from charge states between 0 and 2. The feature due to the decay of the K vacancy in collisions involving F^{8+} appears to be shifted to slightly higher energies when compared to those of F^{7+} and F^{8+}. It was argued[20] that this shift occurs since the KLL Auger decay for a vacancy created in the collision is constrained to take place late in the neutralization process. The systematic difference between the KLL features observed for projectiles carrying an initial K-shell vacancy and those for which the vacancies are produced by the collision indicates the different stages of neutralization of the incident F ion at the time of the Auger decay and hence serves as a time resolved probe of the neutralization process.

DEFINING INCIDENT TRAJECTORIES

It is clear in these experimental measurements that a well defined incident trajectory is important. If the incident ion's energy and angle of incidence fall outside the regime for planar channeling, then the ion can interact with target atoms in close collisions, producing many interesting signatures in the electron energy distributions. Both the observation of target peaks and the production of inner-shell vacancies on the projectile are qualitative evidence for these close collisions. The observed energy threshold for the production of inner-shell vacancies may quantify the distance of closest approach.

Recently, the angular distributions of electrons emitted for 70 keV O^{7+} incident at 30° on Au (see inset Fig. 7) were measured at Oak Ridge. Electron energy distributions were measured at various emission angles, θ, to the surface and the relative intensity of the Auger electrons associated with the 69 eV target NVV transition are presented in Fig. 7. Detailed interpretation of the angular distribution of the total yield and KLL electrons awaits verification that their distributions are not influenced by possible geometrical misalignment of the analyzer as it is rotated to different angles θ. The angular distribution of the target lines shows large oscillations in angle,

which are not observed in either the total or projectile KLL electron emission. These oscillations are in contrast, for example, to the isotropic emission that one would expect from sputtered atoms. Even though these measurements are preliminary it is interesting to compare these results to previous measurements of the angular distribution of Auger electrons emitted from a Cu single crystal in the filling of vacancies created in the solid by a 350 eV electron beam.[27] The oscillations observed in that experiment were explained as resulting from diffraction by lattice atoms of the 62 eV target Auger electrons that have been emitted from several layers beneath the surface. If the same diffraction effects are producing the oscillations in the present measurements, then this observation indicates that several layers of the target crystal are sampled by the incident ions.

ACKNOWLEDGMENTS

The authors would like to thank C. Bottcher, U. Wille, N. Stolterfoht, and J. Burgdörfer for valuable discussions. This work was supported by the Division of Chemical Sciences, U.S. Department of Energy, under Contract No. DE-AC05-840R21400 with Martin Mariettal Energy Sysems, Inc..

▽Lawrence Livermore National Laboratory, Livermore, California 94550.

♠ Permanent Address: Department of Physics, University of Osnabrück, 4500 Osnabrück, Federal Republic of Germany.

References

[1]F. W. Meyer. *Nucl. Instrum. Methods in Phys. Res.*, B9:532, 1985.

[2]E. J. Sternglass. *Phys. Rev.*, 108:1, 1954.

[3]P. Varga. *Invited Papers of XV ICPEAC, Brighton, UK*, 793, 1988.

[4]D. S. Gemmell. *Rev. of Mod. Phys.*, 46:129, 1974.

[5]G. Lakitis, F. Aumayr, and H. Winter. *Proceedings of the International Conference on the Physics of Multicarged Ions, Grenoble, France*, Sept. 12-16, 1988.

[6]D. Schneider and N. Stolterfoht. *Phys. Rev. A*, 19:55, 1979.

[7]D. Schneider, W. C. Werner, N. Stolterfoht, R. J. Fortner, and D. Ridder. *J. Phys. (Colloq.)*, 40:C1–239, 1979.

[8]H. J. Andrae. Proceedings of the nato summer school on fundamental processes of atomic dynamics. *(Maratea, Italy, 21 Sept-2 Oct, 1987), edited by J. S. Briggs*, Plenum Press, 1988.

[9]K. J. Snowdon. *Verhandlungen der Deutschen Physikalischen Gesellschaft*, 7:39, 1988.

[10]F. W. Meyer. *Proceedings of the International Conference on the Physics of Multicarged Ions, Grenoble, France.*

[11]U. A. Arifov, L. M. Kishinevskii, E. S. Mukhamadiev, and E. S. Parilis. *Sov. Phys. Tech. Phys.*, 18:118, 1973.

[12]M. Delaunay, M. Fehringer, R. Geller, D. Hitz, P. Varga, and H. Winter. *Phys. Rev. B*, 35:4232, 1987.

[13]M. Fehringer, M. Delaunay, R. Geller, P. Varga, and H. Winter. *Nucl. Instrum. Methods in Phys. Res.*, B23:245, 1987.

[14]D. M. Zehner, S. H. Overbury, C. C. Havener, F. W. Meyer, and W. Heiland. *Surf. Sci.*, 178:359, 1986.

[15]S. T. de Zwart. Phd thesis, university of groningen, the netherlands. 1987.

[16]M. Delaunay, M. Fehringer, R. Geller, P. Varga, and H. Winter. *Europhys. Letts.*, 4:377, 1987.

[17]F. W. Meyer, C. C. Havener, K. J. Snowdon, S. H. Overbury, D. M. Zehner, and W. Heiland. *Phys. Rev. A*, 35:3176, 1987.

[18]D. Gregory, G. H. Dunn, R. A. Phaneuf, and D. H. Crandall. *Phys. Rev. A*, 20:410, 1979.

[19]K. J. Snowdon, C. C. Havener, F. W. Meyer, D. M. Zehner, and W. Heiland. *Rev. Sci. Instrum.*, 59:902, 1988.

[20]C. C. Havener, K. Reed, K. J. Snowdon, N. Stohlterfoht, D. M. Zehner, and F. W. Meyer. ***submitted to Surface Science Letters.***

[21]K. J. Snowdon. ***Nucl. Instrum. Methods in Phys. Res.***, B34:309, 1988.

[22]P. Apell. ***Nucl. Instrum. Methods in Phys. Res.***, B23:242, 1987.

[23]L. Folkerts and R. Morgenstern. ***Proceedings of the International Conference on the Physics of Multicarged Ions, Grenoble, France,*** Sept. 12-16, 1988.

[24]R. D. Cowan. *The Theory of Atomic Structure and and Spectra.* University of California Press, Berkeley, 1981.

[25]J. Eichler, U. Wille, B. Fastrup, and K. Taulberg. *Phys. Rev. A*, 14:707, 1976.

[26]J. Eichler and U. Wille. *Phys. Rev. A*, 11:1973, 1975.

[27]J. R. Noonan, D. M. Zehner, and L. H. Jenkins. *J. Vac. Sci. Tech.*, 13:183, 1976.

Figures

FIG. 1. Electron energy distributions[17] for 60 keV N^{4+}, N^{5+}, and N^{6+} projectiles incident on Au(110) at 5°. The experimental geometry is shown in an inset.

FIG. 2. Secondary electron energy spectra for Ar^{q+} on tungsten for several projectile energies. (Fig. taken from the thesis of de Zwart)

FIG. 3. Electron energy distributions for 70 keV O^{7}+ ions incident on Au, for six different angles of incidence. Horizontal lines under the O KLL peaks give ranges of KLL transition energies for all charge states $\leq 5+$.

FIG. 4. Correlation diagram for the N-Au system.

FIG. 5. The electron energy distributions for F^{q+} on Cu.

FIG. 6. Molecular orbital diagram constructed for the F^{2+} - Cu system. The smallest internuclear separations correspond to the united atom limit while the largest approach the separate atom limit.

FIG. 7. Angular distributions of the 69 eV target, KLL Auger, and total electrons emitted for 70 keV O^{7+} incident at 30° on Au.

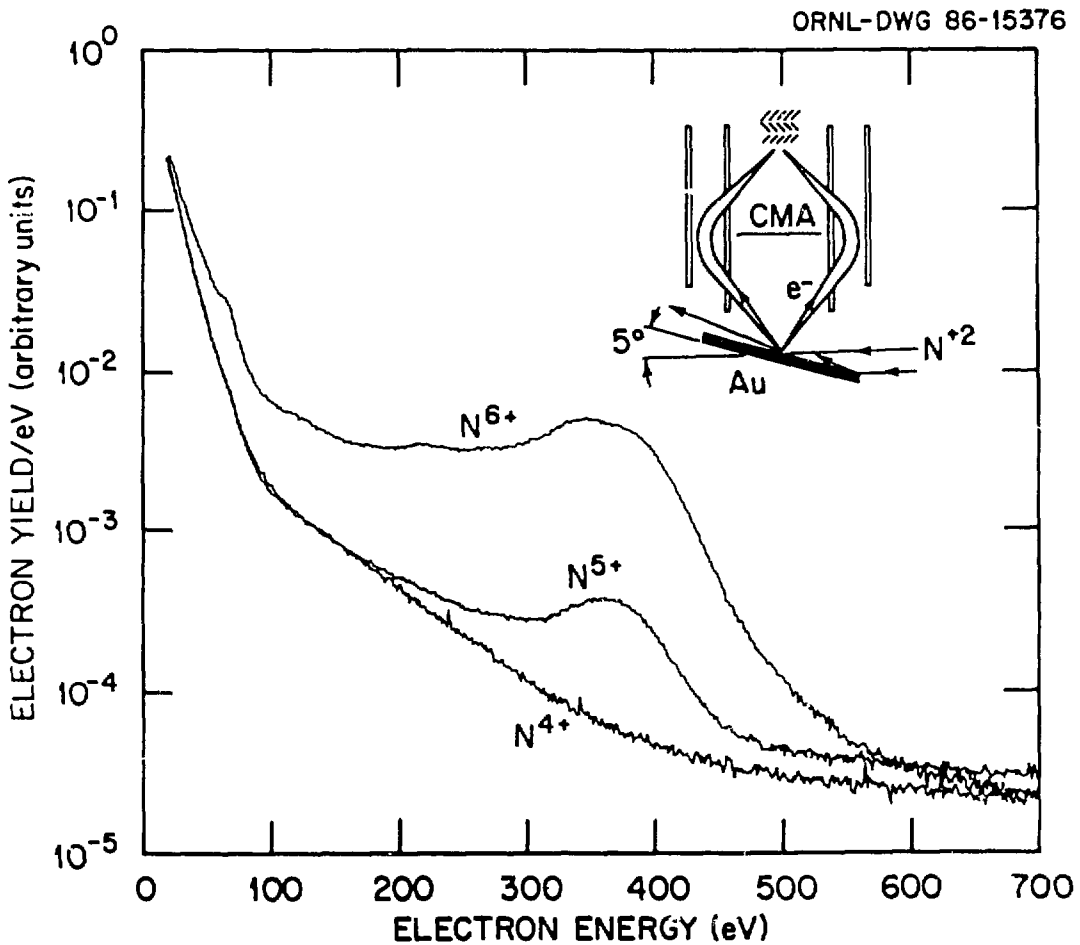
ORNL-DWG 86-15376
ELECTRON YIELD/eV (arbitrary units)
ELECTRON ENERGY (eV)
10^0
10^{-1}
10^{-2}
10^{-3}
10^{-4}
10^{-5}
0
100
200
300
400
500
600
700
N^{6+}
N^{5+}
N^{4+}
CMA
e^-
5°
N^{+2}
Au

Fig. 1

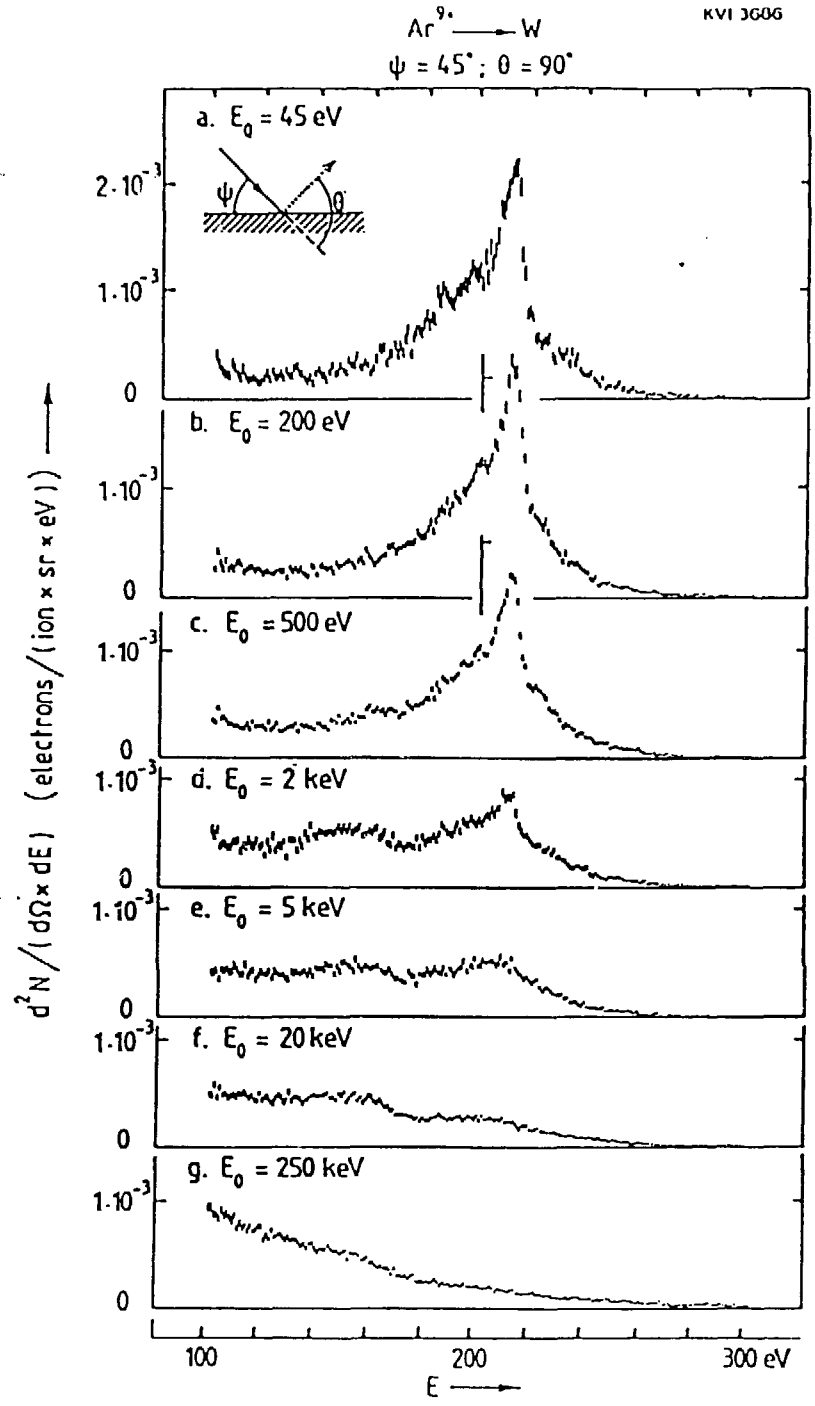
KVI 3606
$Ar^{9+} \longrightarrow W$
$\psi = 45^\circ$; $\theta = 90^\circ$
a. E_0 = 45 eV
b. E_0 = 200 eV
c. E_0 = 500 eV
d. E_0 = 2 keV
e. E_0 = 5 keV
f. E_0 = 20 keV
g. E_0 = 250 keV
ψ
θ
$2 \cdot 10^{-3}$
$1 \cdot 10^{-3}$
0
$d^2N/(d\Omega \times dE)$ (electrons/(ion × sr × eV)) ⟶
100
200
300 eV
E ⟶

Fig. 2

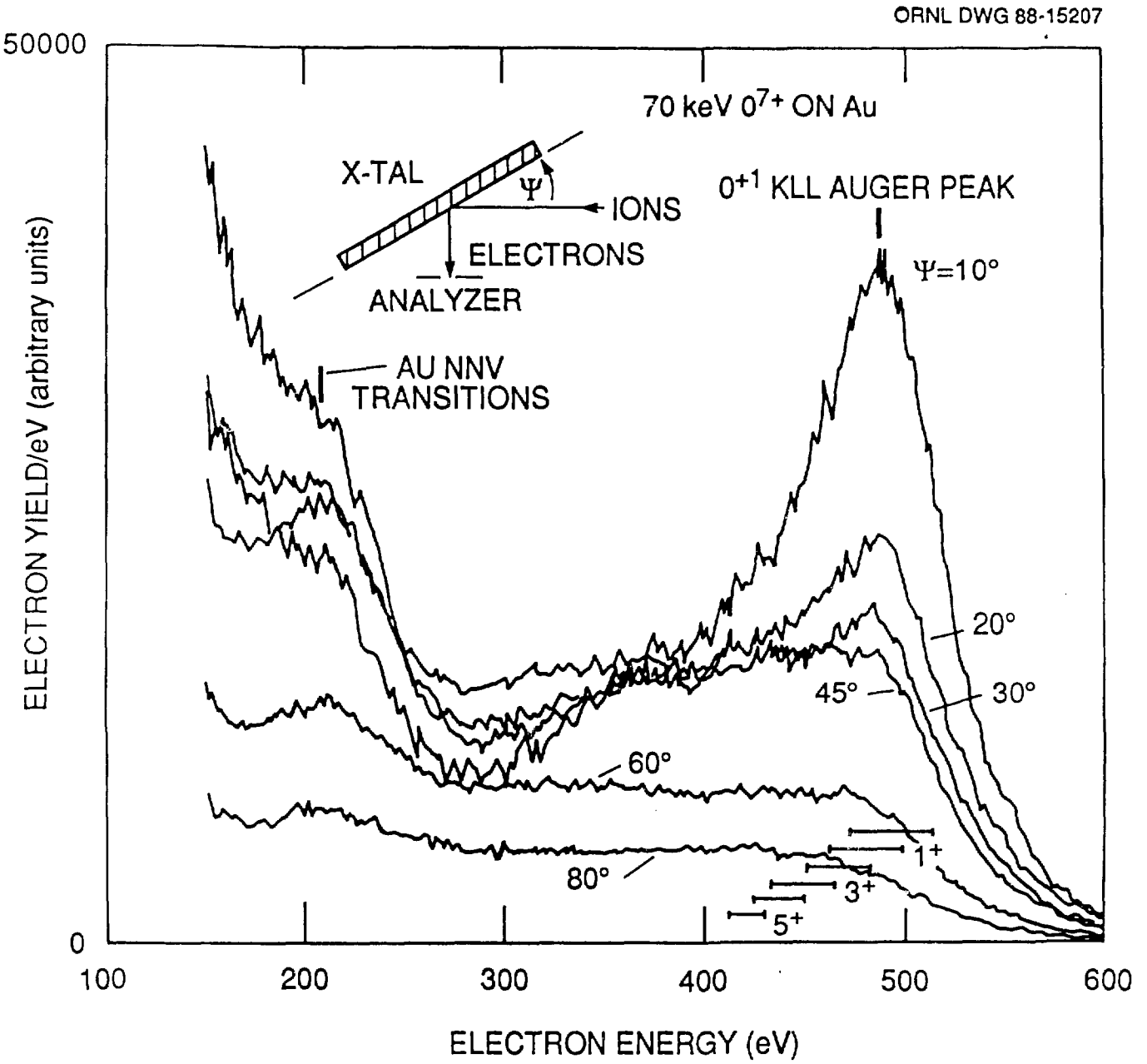
ORNL DWG 88-15207
50000
0
70 keV 0^{7+} ON Au
X-TAL
Ψ
IONS
ELECTRONS
ANALYZER
0^{+1} KLL AUGER PEAK
Ψ=10°
AU NNV
TRANSITIONS
20°
30°
45°
60°
80°
1+
3+
5+
ELECTRON YIELD/eV (arbitrary units)
100
200
300
400
500
600
ELECTRON ENERGY (eV)

Fig. 3

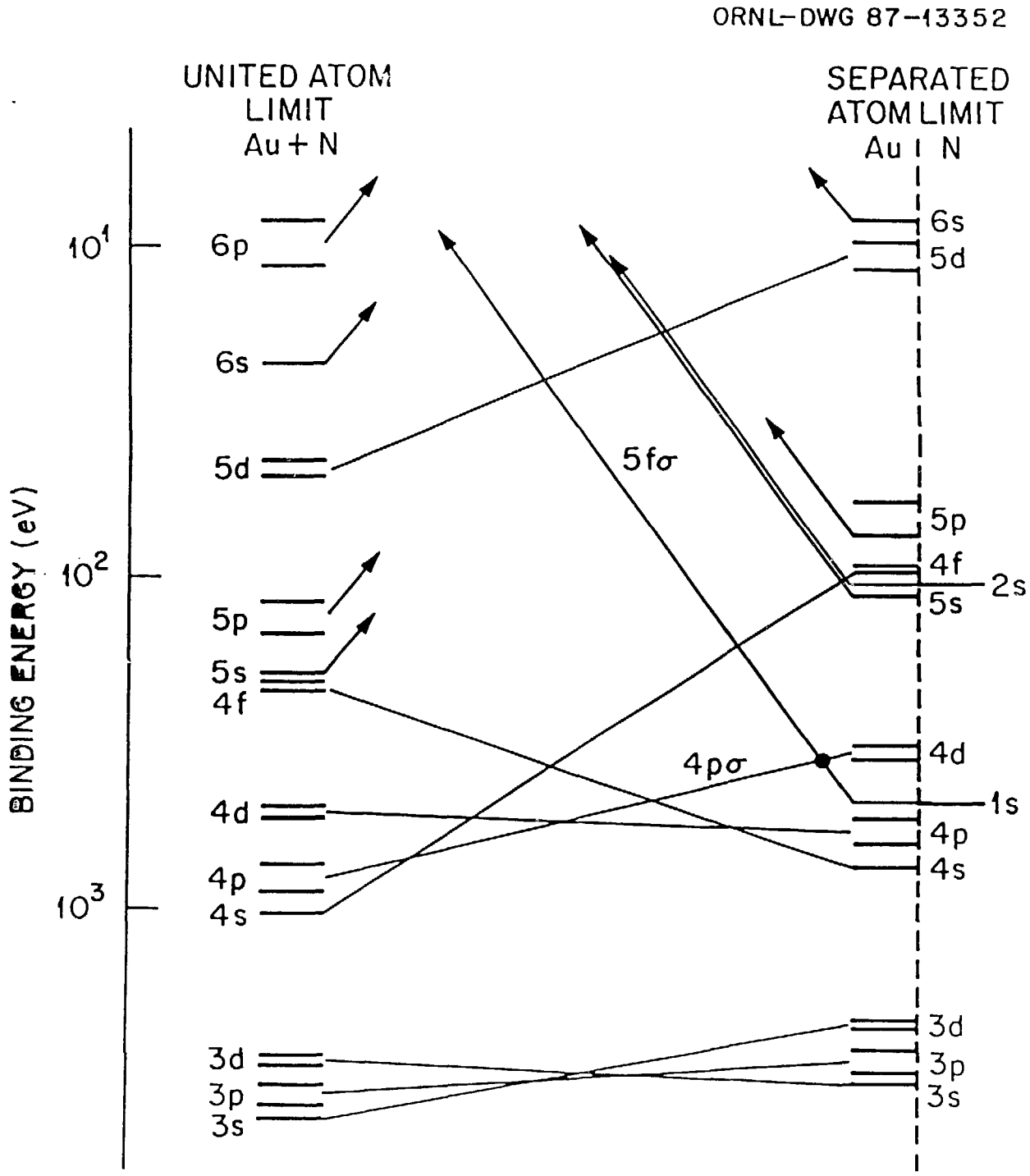
ORNL-DWG 87-13352
UNITED ATOM LIMIT Au + N
SEPARATED ATOM LIMIT Au + N
BINDING ENERGY (eV)
10^1
10^2
10^3
6p
6s
5d
5p
5s
4f
4d
4p
4s
3d
3p
3s
5fσ
4pσ
6s
5d
5p
4f
5s
2s
4d
1s
4p
4s
3d
3p
3s

Fig. 4

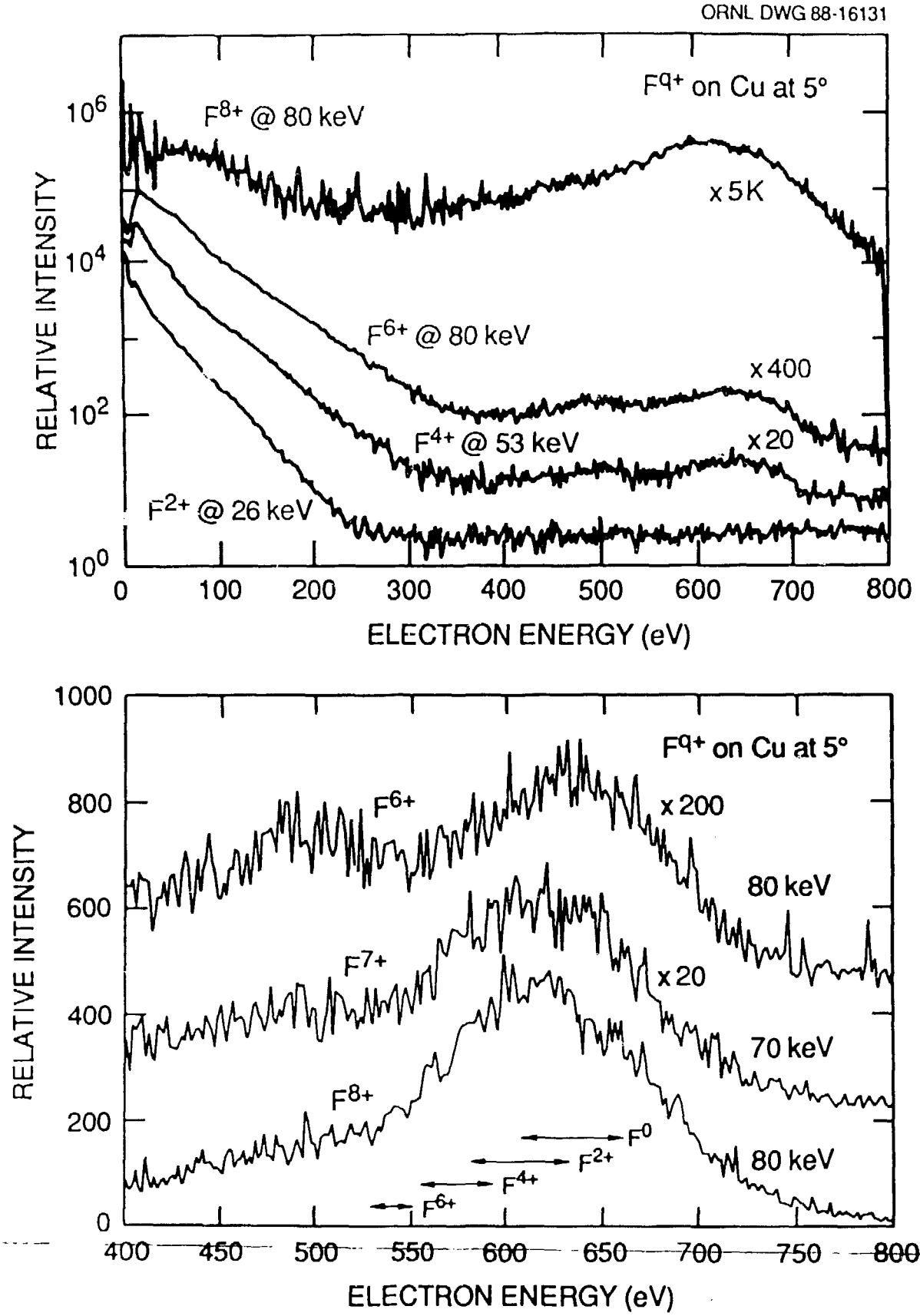
ORNL DWG 88-16131
F^{q+} on Cu at 5°
F^{8+} @ 80 keV
x 5K
F^{6+} @ 80 keV
x 400
F^{4+} @ 53 keV
x 20
F^{2+} @ 26 keV
RELATIVE INTENSITY
10^6
10^4
10^2
10^0
0 100 200 300 400 500 600 700 800
ELECTRON ENERGY (eV)
F^{q+} on Cu at 5°
F^{6+}
x 200
80 keV
F^{7+}
x 20
70 keV
F^{8+}
F^0
F^{2+}
F^{4+}
F^{6+}
80 keV
RELATIVE INTENSITY
1000
800
600
400
200
0
400 450 500 550 600 650 700 750 800
ELECTRON ENERGY (eV)

Fig. 5

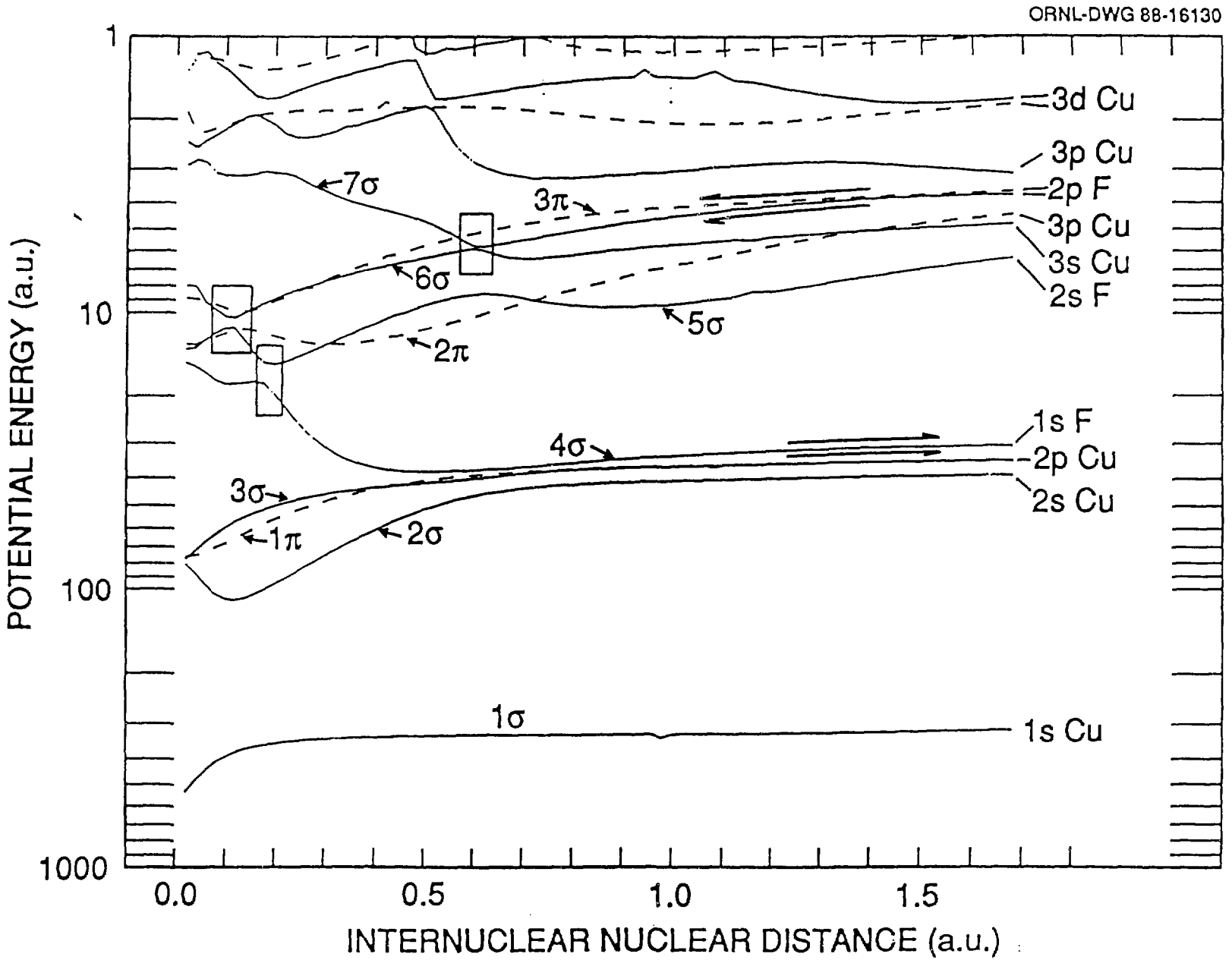
ORNL-DWG 88-16130
POTENTIAL ENERGY (a.u.)
1
10
100
1000
0.0
0.5
1.0
1.5
INTERNUCLEAR NUCLEAR DISTANCE (a.u.)
3d Cu
3p Cu
2p F
3p Cu
3s Cu
2s F
1s F
2p Cu
2s Cu
1s Cu
7σ
3π
6σ
5σ
2π
4σ
3σ
1π
2σ
1σ

Fig. 6

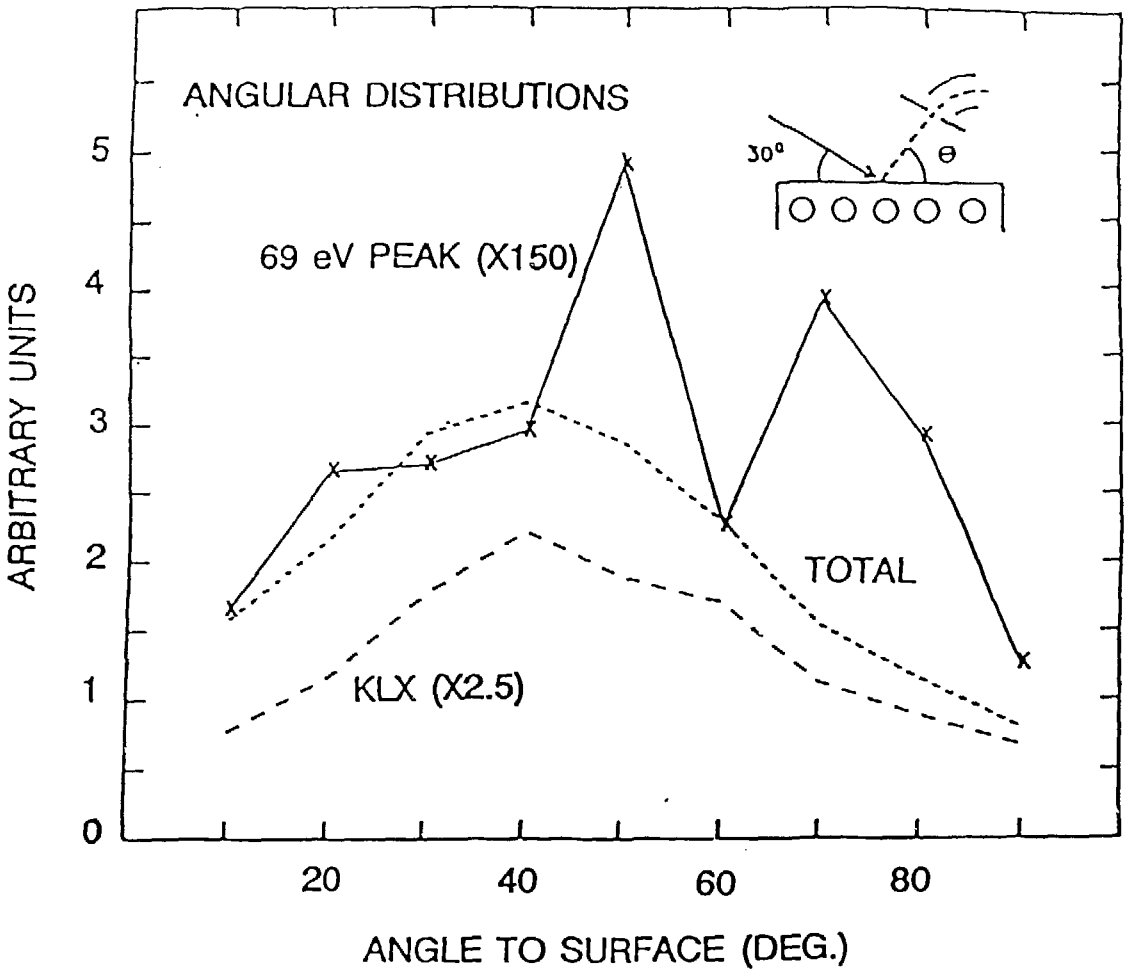
ANGULAR DISTRIBUTIONS
30°
θ
69 eV PEAK (X150)
TOTAL
KLX (X2.5)
ARBITRARY UNITS
0
1
2
3
4
5
20
40
60
80
ANGLE TO SURFACE (DEG.)

Fig. 7